

## Table-top X-ray microscopy: Sources, optics and applications

H.M. Hertz, G.A. Johansson, H. Stollberg, J. de Groot, O. Hemberg, A. Holmberg, S. Rehbein, P. Jansson, F. Eriksson<sup>1</sup> and J. Birch<sup>1</sup>

*Biomedical and X-Ray Physics, Royal Institute of Technology (SCFAB), 10691 Stockholm, Sweden*

<sup>1</sup> *Department of Physics (IFM), Linköping University, 58183 Linköping, Sweden*

**Abstract.** We have developed the first operative compact sub-visible-resolution x-ray microscope for the water-window region ( $\lambda = 2.3 - 4.4$  nm). The microscope is based on a 100 Hz liquid-jet-target laser-plasma x-ray source, normal-incidence multilayer condenser optics, diffractive zone plate optics and CCD detection. In the present article we emphasize the system's aspects and summarize the recent progress on the components, all aiming at the reduction of the exposure time of a few seconds, i.e., similar to bending-magnet based microscopes. This primarily includes improved laser-plasma source, improved condenser optics using Cr/Sc multilayers, and improved image handling capability using wavelet algorithms. Such compact short-exposure time microscopes would significantly increase the applicability of the technology.

### 1. INTRODUCTION

X-ray microscopy in the water-window region ( $\lambda=2.3-4.4$  nm) is an attractive technique for high-resolution imaging.<sup>1</sup> In this wavelength region state-of-the-art optics demonstrate sub-20 nm resolution and the sample preparation techniques are maturing. The latter is especially important for wet samples, e.g., cells or other structures, where thick samples may be imaged in their aqueous environment with natural or artificially labeled contrast. Unfortunately all user-friendly operational x-ray microscopes are based on synchrotron radiation sources, which limit their accessibility. Many biological investigators would benefit from having the x-ray microscope as a tool among other tools in their own laboratory. For this purpose we recently demonstrated the first compact x-ray microscope with sub-visible resolution.

In the present paper we describe the further development of compact x-ray microscopy towards an application-oriented instrument. We discuss recent improvements in the different subsystems and emphasize system aspects, i.e., the interaction between the different x-ray components of the microscope. The overall goal is to reduce the exposure time to a few seconds.

### 2. THE COMPACT X-RAY MICROSCOPE

The compact full-field microscope is based on a liquid-jet target laser-plasma x-ray source, normal-incidence multilayer condenser optics, diffractive zone plate optics and CCD detection<sup>2,3</sup>. The source is a 100 Hz, negligible-debris, high-brightness ethanol liquid-jet laser-plasma source providing  $\lambda=3.37$  nm radiation from carbon-ion emission with narrow line width. A normal-incidence spherical W/B<sub>4</sub>C multilayer mirror operates as condenser and illuminates the sample. The high-resolution imaging is currently performed with a ~7% efficient nickel zone plate with an outermost zone width of 40 nm. Detection is performed with a back-illuminated CCD camera with a pixel size of  $24 \times 24 \mu\text{m}^2$ .

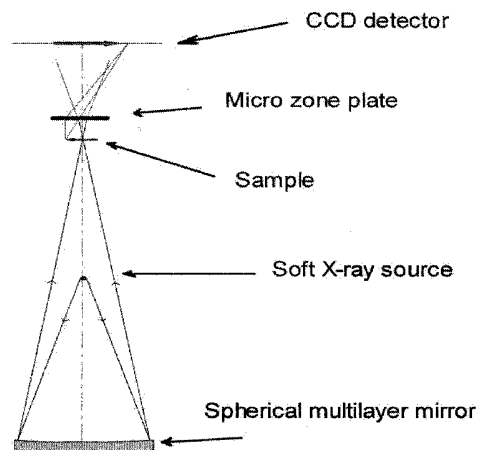


**Figure 1:** Principle setup of the compact x-ray microscope

### 3. LASER-PLASMA SOURCE

The prime requirement for a compact x-ray microscope is a compact source. We use an incoherent laser-plasma source based on a continuous liquid-jet target.<sup>4,5</sup> The generic arrangement is shown in Fig 2. A  $\sim 10 \mu\text{m}$  diam. liquid jet is formed inside an  $\sim 10^{-3}$  mbar pressure vacuum chamber by forcing the ethanol through a small glass capillary nozzle. The jet eventually breaks up into droplets due to the liquid's tendency to minimize surface energy. The 100 Hz, 3 ns SHG Nd:YAG laser is focused on the jet before it breaks up in droplets with a focal spot diameter close to the diameter of the target. Due to the small target and focus size, the laser pulse energy can be kept at a reasonable level while still achieving sufficient intensity in the focused spot to produce plasma temperatures suitable for water-window x-ray generation. The microscope operates at the  $\lambda=3.37 \text{ nm}$  C VI emission line

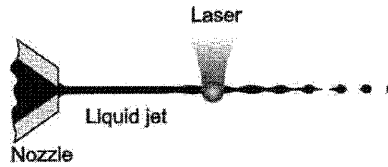


Fig. 2. Experimental arrangement for liquid-jet laser-plasma source

This regenerative target type provides fresh target material at liquid density for full-day operation without interrupts. It allows high-repetition-rate lasers to be used, thereby having potential for high average power. Furthermore, it reduces debris production several orders of magnitude compared to conventional targets and for certain liquids debris is practically eliminated.<sup>6</sup> Thus, the effective photon flux may be increased a few orders of magnitude compared to conventional targets since collection optics may be used reasonably close to the plasma. By choosing a suitable target liquid, the emission wavelength may be spectrally tailored to suit, e.g., x-ray microscopy or EUV lithography.<sup>7,8</sup>

The major issues as regards the source from the microscope system's perspective is stability, reliability, brightness, and wavelength.

We have chosen to operate the source in the microscope in the liquid-jet mode as opposed to the droplet mode in order to increase stability by avoiding fluctuations in the x-ray flux due to droplet drift. However, given the high surface tension of ethanol, the distance between the nozzle and the plasma is too short with the previously used nozzles (1-2 mm). A new nozzle fabrication method, based on glass capillaries<sup>9</sup>, allows us to operate at higher pressure and larger jet diameters, thereby increasing the distance to the drop formation point, and thus the nozzle-plasma distance, to a few mm. More important, the new nozzles allows optimization of the target diameter to the laser pulse, resulting in an increase in the emitted flux of  $>4\times$ . This is described by de Groot et. al. in Ref. 10. We estimate that the gain in brightness and, thus, reduction in exposure time will be a factor 2-3 with this method.

In a parallel project we are developing a stable source for compact microscopy in the lower wavelength range of the water-window. Microscopy at such wavelengths allows transmission through thicker samples and is thus important for many cell studies. We have previously shown that a liquid nitrogen jet provides emission at suitable wavelengths  $\lambda=2.48$  or  $\lambda=2.88 \text{ nm}$ .<sup>11</sup> However, the jet did not have the necessary stability and reliability to allow microscopy. We have recently used the new nozzles for producing a stable jet of liquid nitrogen in vacuum. Figure 3 shows a  $9.5 \mu\text{m}$  diam jet photographed by a 4 ns Nd:YAG laser illumination. The jet has been operated several hours without instabilities.

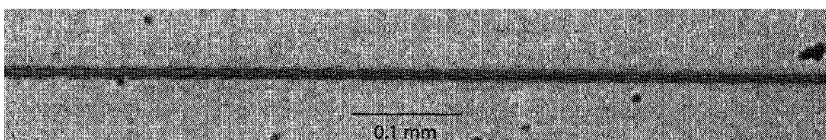


Figure 3. Image of stable  $9.5 \mu\text{m}$  diam liquid nitrogen jet approximately 3.5 mm from the nozzle orifice.

#### 4. MULTILAYER CONDENSER

Given the fact that we employ an incoherent  $4\pi$ -emitting source, the collection efficiency of the condenser system is of outmost importance for reasonable exposure times. The compact x-ray microscope uses a normal-incidence multilayer mirror to focus the small high-brightness source on the sample plane.<sup>12</sup> In addition to providing smaller aberration than, e.g., elliptical mirrors, this condenser concept automatically monochromatizes the incoming radiation, something that is important due to the large chromatic aberration of the imaging zone plate optics. The current condenser optics is based on 200 bilayers of W/B<sub>4</sub>C on a 58 mm diam spherical substrate with a radius of curvature of 343 mm. The average reflectivity at  $\lambda=3.374$  nm is  $\sim 0.5\%$  with a peak reflectivity at certain positions of up to 3%. Note that the fabrication is a very challenging deposition problem: Not only does one require high reflectivity, in addition the multilayer d-spacing must match the wavelength of the selected line in the line-emitting source – and that match should be over a large area.

Still, from a system's perspective, the multilayer mirrors are advantageous. The normal-incidence operation results in small aberrations and, thus, simple alignment. The two major problems with the system are the low reflectivity and the flare. The reflectivity is primarily a function of materials and surface roughness. We choose to investigate the Cr/Sc system, which show extremely high theoretical reflectivity assuming perfect interfaces ( $\sim 64\%$  at  $\lambda=3.115$  nm and  $40\%$  at  $\lambda=3.374$  nm).<sup>13</sup> In parallel we developed a compact angular-scanning reflectometer allowing us to perform in-house measurements of d-spacing and reflectivity.<sup>14</sup>

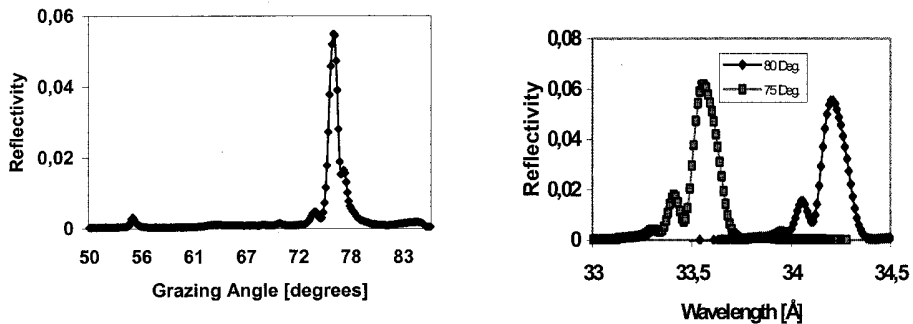


Fig. 4. Comparative measurements of reflectivity of Cr/Sc multilayer with the compact angle-tuned reflectometer at  $\lambda=3.374$  nm (left) and the wavelength-tuned reflectometer at ALS (right).

We use ion-assisted dual-target magnetron sputtering to grow the Cr/Sc multilayer structures. The goal is the fabrication of a d-spacing for normal-incidence reflectivity at the  $\lambda=3.374$  nm line and for the Sc absorption edge. In order to stimulate the ad-atom mobility and improve the interface flatness, the multilayers were intentionally irradiated with Ar ions with varying ion energies ( $\sim 0-40$  eV) during growth. Hard x-ray reflectivity measurements on multilayers grown with different ion energies revealed an optimum at an ion energy of 24 eV. At this optimum, the at-wavelength reflectivity ( $\lambda=3.374$  nm) was measured to 5.5% at a grazing-incidence angle of  $76^\circ$  for a multilayer with 400 bilayers. The measurements were performed by the compact reflectometer and later confirmed at ALS (cf. Fig. 4). For multilayers grown for the highest reflectivity at the scandium edge, two multilayers with 600 bilayers each, show excellent performance. Measurements at ALS reveal a near-normal incidence ( $\lambda=87.5^\circ$ ) reflectivity of 14.6%, a significant improvement compared to previous results.<sup>15</sup> Simulations of the synchrotron radiation data using the IMD software resulted in interface widths of 0.38-0.41 nm.

Two major issues remain to be resolved as regards the Cr/Sc condenser mirror: The high-reflectivity coatings have to be uniformly deposited over a large diameter substrate and flare has to be measured and reduced. Finally, it should be noted that our initial work on Ni/V mirrors for  $\lambda=2.48$  nm normal-incidence reflectivity show significant promise. Preliminary measurements on a 500 bi-layer mirror indicate  $>2\%$  reflectivity at near-normal incidence ( $86^\circ$ ).<sup>16</sup>

## 5. DIFFRACTIVE OPTICS

Zone plates, gratings and similar structures are essential for x-ray microscopy for the high-resolution imaging, for spectroscopy and for test objects to characterize the microscopy. The current microscope utilizes a 40 nm outer zone width Ni electro-plated zone plate manufactured in Göttingen.<sup>17</sup> In order to have a greater flexibility as regards zone plate parameters we have started an in-house nano fabrication effort based on electroplated nickel. A plating mold is produced from a tri-layer system on 50 nm SiN membranes with a 10 nm Cr + 15 nm Ge plating base. The three layers typically are, from bottom to top, 140 nm ARC XL-20, 5 nm Ti and 40 nm Zep. The plating mold is then structured by subsequent steps of e-beam lithography (Raith 150) and RIE with  $\text{BCl}_3$  and  $\text{O}_2$  (Oxford Plasmalab 80+). To get the final structure, nickel is plated and the plating mold is removed by RIE. Figure 5 shows electroplated Ni lines at different line widths. The typical height of Ni is  $>110$  nm.

This process will be used for fabricating zone plates in house. To date it has only been used for test objects, as will be discussed in the next section.

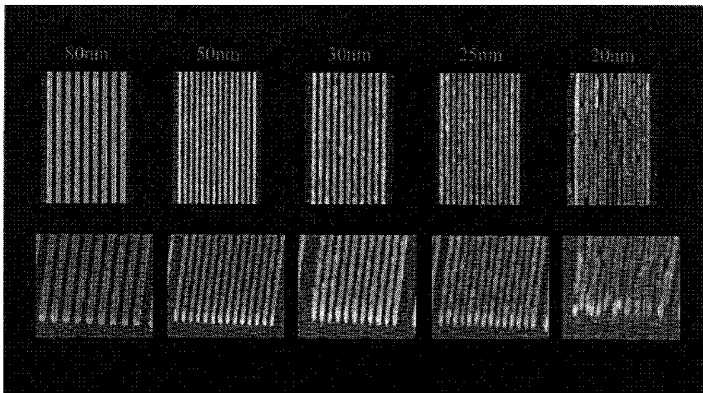


Fig. 5. Electroplated nickel with  $L/S=1$  for different line widths

## 6. IMAGING

The compact x-ray microscope has demonstrated imaging of test structures, diatoms, dry COS-7 cells, colloidal gold etc.<sup>3,4</sup> Figure 6 shows an image of a 50 and 60 nm  $L/S$  Ni grating fabricated in house. The 60 nm  $L/S$  show good contrast while the 50 nm  $L/S$  are visible but with less contrast. The exposure time is 1 min. This is somewhat longer than previously due to a slow degeneration of one of our condenser mirrors.

Figure 6 illustrates the major imaging problem with the compact XRM: low contrast due to noise. Given the lower power of the compact source and the restriction against prohibitive long exposure times, images will be noisy. We have recently developed a denoising method based on the wavelet transform that shows excellent results. Typically the exposure time can be reduced a factor 2 without reduction of image quality. The method is described by Stollberg et. al. in the present volume.<sup>18</sup>

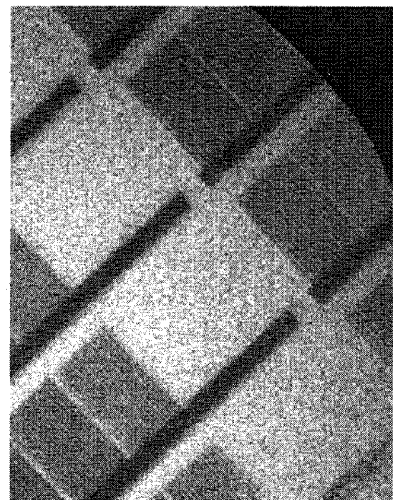


Fig. 6. Image of test grating with with 50 nm  $L/S$  (lower left) and 60 nm  $L/S$  (upper right).

The noise does, however, have different components. Part of the noise has been identified as scattered x-rays due to the mid-spatial-frequency flare in the multilayer condenser mirror. Naturally this noise is also reduced by the wavelet denoising but will be more effectively removed by eliminating the flare of the mirror and other scattering elements. As a partial remedy a pinhole has been introduced between the zone plate and the sample.

## 7. DISCUSSION

As demonstrated in the present paper, compact x-ray microscopy can be performed with reasonable exposure times (typically 1-5 minutes) at  $\lambda=3.37$  nm. However, as discussed above there is room for improvement. In summary, the source optimization may result in 2-3 $\times$  reduction, higher multilayer reflectivity 10  $\times$ , reduction of multilayer flare 3 $\times$ , and wavelet denoising 2 $\times$ . In addition, a laser with higher average power could certainly yield 5  $\times$ . Given that these improvements can be implemented in the microscope, we would be able to perform exposure times on the order of 1 second of dry samples, an exposure time similar to that of bending-magnet-based microscopes.

Of equal importance as the shorter exposure time is the reduction of operating wavelength to the nitrogen emission lines at 2.48 nm and 2.88 nm. At these wavelengths the transmission of the samples is significantly higher, making imaging of thicker samples possible. As discussed above the source for this wavelength seems to reach sufficient stability to allow integration in a microscope. The condenser optics may either be a condenser zone plate<sup>19</sup> or multilayer mirrors. Recent results on Ni/V multilayer mirrors show promise for 1-2% reflectivity, which in combination with the higher sample transmission at these wavelengths can be projected to few-second exposure times.

## Acknowledgments

The authors are grateful to Eric Gullikson for ALS measurements, Markus Peuker for the zone plates, and Magnus Berglund for his contributions.

## References

- <sup>1</sup> J. Kirz, C. Jacobsen, and M. Howells, *Q. Rev. Biophys.* **28**, 33 (1995); G. Schmahl, D. Rudolph, B. Niemann, P. Guttman, J. Thieme, G. Schneider, M. Diehl, and T. Wilhein, *Optik* **93**, 66 (1993).
- <sup>2</sup> M. Berglund, L. Rymell, M. Peuker, T. Wilhein, and H. M. Hertz, *J. Microscopy* **197**, 268 (2000)
- <sup>3</sup> G. Johansson, A. Holmberg, H. M. Hertz, and M. Berglund, *Rev. Sci. Instrum.* **73**, 1193 (2002).
- <sup>4</sup> L. Rymell and H.M. Hertz, *Opt. Commun.* **103**, 105 (1993).
- <sup>5</sup> L. Malmqvist, L. Rymell, M. Berglund and H.M. Hertz, *Rev. Sci. Instrum.* **67**, 4150 (1996).
- <sup>6</sup> L. Rymell and H.M. Hertz, *Rev. Sci. Instrum.* **66**, 4916 (1995).
- <sup>7</sup> L. Rymell, M. Berglund and H.M. Hertz, *Appl. Phys. Lett.* **66**, 2625 (1995); M. Berglund, L. Rymell, and H. M. Hertz, *Appl. Phys. Lett.* **69**, 1683 (1996).
- <sup>8</sup> B.A.M. Hansson, L. Rymell, M. Berglund, and H.M. Hertz, *Microel. Engin.* **53**, 667 (2000).
- <sup>9</sup> J. de Groot, G.J. Johansson, and H.M. Hertz, submitted to *Rev. Sci. Instrum* (2002).
- <sup>10</sup> J. de Groot, G. A. Johansson, O. Hemberg, and H. M. Hertz, this volume.
- <sup>11</sup> M. Berglund, L. Rymell, T. Wilhein, and H.M. Hertz, *Rev. Sci. Instrum.* **69**, 2361 (1998).
- <sup>12</sup> H. M. Hertz, L. Rymell, M. Berglund, G. Johansson, T. Wilhein, Y. Platonov, and D. Broadway, in *X-ray Optics, Instruments, and Missions II*, Proc. SPIE **3766**, 247 (1999)
- <sup>13</sup> J. Birch, F. Eriksson, G. J. Johansson, and H. M. Hertz, *Vacuum* **68**, 65 (2002)
- <sup>14</sup> G. A. Johansson, M. Berglund, J. Birch, F. Eriksson, and H. M. Hertz, *Rev. Sci. Instrum.* **72**, 58 (2001).
- <sup>15</sup> F. Eriksson, J. Birch, E. M. Gullikson, G. A. Johansson, and H. M. Hertz, in preparation for *Opt. Lett.*
- <sup>16</sup> F. Eriksson et. al., manuscript in preparation.
- <sup>17</sup> M. Peuker, *Appl. Phys. Lett.* **78**, 2208 (2001).
- <sup>18</sup> H. Stollberg, J. Boutet de Monvel, G.A. Johansson, and H.M. Hertz, this volume.
- <sup>19</sup> G. Schneider, personal communication.